Appl Biochem Biotechnol (2008) 144:27–36
DOI 10.1007/s12010-007-8002-5

Cytochrome P450 BM-3 Evolved by Random and Saturation Mutagenesis as an Effective Indole-Hydroxylating Catalyst

Hong-mei Li · Le-he Mei · V. B. Urlacher · R. D. Schmid

Received: 15 April 2007 / Accepted: 13 June 2007 /
Published online: 27 November 2007

Abstract Cytochrome P450 BM-3 with the mutations A74G, F87V, and L188Q could catalyze indole to produce indigo and indirubin. To further enhance this capability, site-directed and random mutageneses on the monooxygenase domain of P450 BM-3 mutant (A74G/F87V/L188Q; 3X) were performed. The mutant libraries created by error-prone polymerase chain reaction were screened using a colorimetric colony-based method on agar plates followed by a spectroscopic assay involving in absorption of indigo at 670 nm and NADPH at 340 nm in microtiter plate. Three mutants (K434R/3X, E435D/3X, and D168N/A225V/K440N/3X) exhibited higher hydroxylation activity toward indole in comparison to parent enzyme. Moreover, using saturation site-directed mutagenesis at amino acid positions 168, 225, 434, 435, and 440, two P450 BM-3 variants (D168H/3X, E435T/3X) with an up to sixfold increase in catalytic efficiency (k_{cat}/K_m) were identified, and the mutant D168H/3X acquired higher regioselectivity resulting in more indigo (dimerized 3-hydroxy-indole) compared to parent mutant (93 vs72%).

Keywords Cytochrome P450 monooxygenase · Error-prone PCR · Indole · Indigo · Saturation mutagenesis · P450 BM-3

H.-m. Li (✉) · L.-h. Mei
Department of Chemical and Biochemical Engineering, Zhejiang University, Hangzhou 310027, China
e-mail: Eastshine@21cn.com

H.-m. Li
Institute of Food Science and Biological Technology, University of Shanghai for Science and Technology, Shanghai 200093, China

V. B. Urlacher · R. D. Schmid
Institute of Technical Biochemistry, University of Stuttgart, 70569 Stuttgart, Germany

Introduction

Indigo is a widely used dye, and its synthesis played a critical role in development of the chemical industry in the nineteenth century [1, 2]. Until nowadays, chemical synthesis dominates in indigo production [3]. However, that the chemically synthesized indigo provoked the environmental pollution has urged scientists to seek for a green alternative for indigo production. Several microbial dioxygenases have been found to oxidize indole into 3-hydroxy-indole, which spontaneously forms indigo [4, 5], and this reaction catalyzed by a bacterial naphthalene dioxygenase expressed in *Escherichia coli* was utilized for a process development [6, 7].

An alternative approach is oxidation of indole by a suitable cytochrome P450 monooxygenase with an appropriate specificity. Cytochromes P450s comprise a ubiquitous superfamily of heme-containing enzymes, which is a potentially useful class in catalysis of diverse oxygenation reactions. Recently, CYP2A6, 2C19, and 2E1 [8–10] involved in the detoxification of xenobiotic compounds were found to be entangled in the metabolism of indole leading to indigo. Also, a mutant of cytochrome P450 BM-3 from *Bacillus megaterium* can efficiently hydroxylate indole to the hydroxylated products leading further to indigo and indirubin [11].

P450 BM-3 from *B. megaterium* is a self-sufficient natural fusion protein consisting of a P450 heme monooxygenase and a NADPH-dependent diflavin reductase. This composition is responsible for very high turnover rates, rendering this protein attractive for practical applications. To expand its capability in the oxidization of a wider range of unnatural substrates, the enzyme has been modified by protein engineering [12–17]. Predictions based on crystal structures in the case of the oxidoreductase catalyzed reactions are rather complex because catalytic efficiency and the enzyme specificity are usually connected to loop flexibility that can be affected by a number of factors such as disulfide bridges, prolines in turns, and hydrogen bonding interactions. Compared to rational design, directed evolution, a widely used dynamic tool for protein engineering independent of crystal structures, draws its power from iterative cycles of random mutagenesis and screening of mutants. Combination of random mutagenesis and site-directed mutagenesis is very promising for engineering P450 enzymes with new functions and can be used to enrich the knowledge of the structure–function relationship of these enzymes. The P450 BM-3 with mutations at A74G, F87V, and L188Q (3X) has been obtained by a combination of site-directed and saturation mutagenesis; whereas, we also noted that the triple mutant (3X) produced a side product indirubin, a heterodimer of 2- and 3-hydroxyindole [11] as well as product indigo. Herein, evolution of this enzyme were implemented in terms of further increase of its indole-hydroxylating activity as well as higher regioselectivity by error-prone polymerase chain reaction (PCR) and saturation mutagenesis, with a final aim of more efficient indigo production.

Materials and Methods

Chemicals and Enzymes

All chemicals were of analytical grade or higher quality and purchased from Fluka (Buchs, Switzerland) or Merck (Darmstadt, Germany); restriction endonucleases, T4 DNA ligase, *Taq* DNA polymerase, and *Pfu* DNA polymerase were obtained from Fermentas (Germany).

Bacterial Strains

Escherichia coli DH5a strain was used for collecting the mutant libraries; *E. coli* BL21 (DE3) strain was used for recombinant expression of the P450 monooxygenases. All strains were stored in 50% glycerol at −80 °C and cultivated as recommended by the suppliers.

Creation of P450 BM-3 Mutant Libraries by Error-Prone PCR

Error-prone PCR was performed on the monooxygenase domain of the gene (about 1,466 bp), coding for the triple mutant P450 BM-3(A74G/F87V/L188Q) cloned into the pET28 (a+) vector. A *Bam*HI recognition site was inserted by site-directed mutagenesis between the monooxygenase and the reductase domain, resulting in a silent mutation. Mutagenic buffer (50 μl) was prepared, containing 10 pmol of dNTPs (unbalanced dNTPs), 20 pmol of each primer, about 1 ng of template DNA and $MnCl_2$ in the range of 0–0.2 mM. After denaturation for 3 min at 95 °C, all PCR reactions were repeated 26 cycles (95 °C for 1 min, 47 °C for 2 min, 72 °C for 2 min). After that, the reaction medium was held at 72 °C for 2 min. Subsequent restriction of PCR products and original plasmid with the *Nhe*I and *Bam*HI endonucleases and ligation by T4-DNA ligase were done by standard methods [18]. The ligation mixtures were transformed into *E. coli* DH5a competent cells (Novagen, CA, USA), which was plated on Lauria–Bertani (LB) agar containing kanamycin (30 μg/ml) and incubated overnight at 37 °C. After the addition of 2 ml LB medium, the colonies were scraped and shaken in a thick suspension for 3 h at 37 °C. Plasmid preparation was performed using the QIA prep_ miniprep kit (Qiagen).

Creation of Saturation Site-Directed Mutants

Saturation site-directed mutagenesis was carried out using a few pairs of oligonucleotide primers. The sequences of oligonucleotides were listed in Table 1. The target amino acid positions were coded by NNN, where N = A, G, C, or T. The reactions were carried out as described in the Stratagene Quik Change™ site-directed mutagenesis protocol [19]. After reaction, 10 U of *Dpn*I was added to the products and incubated at 37 °C for 2 h to digest the template DNA.

Table 1 Oligonucleotide sequences used for site-saturation mutagenesis.

Target sites	Oligonucleotide sequences
168	5′-CAGCTTTTACCGA*NNN*CAGCCTCATCC-3′
	5′-GGATGAGGCTG*NNN*TCGGTAAAAGCT-3′
225	5′-GCAGATCGCAAA*NNN*AGCGGTAGCG-3′
	5′-CGCTTTGTTCACCGCT*NNN*TTTGTGC-3′
435	5′-CGAGCTGGATATTA*NNN*AAACTTTAA-3′
	5′-CGTTAAAGTTT*NNN*TAATATCCAGCTC-3′
434	5′-CGAGCTGGATATT*NNN*GAAACTTTAACG-3′
	5′-CGTTAAAGTTTC*NNN*AATATCCAGCTC-3′
440	5′-GAAACTTTAACGTTA*NNN*CCTGAAGG-3′
	5′-CCTTCAGG*NNN*TAACGTTAAAGTTTC-3′

Target amino acid position was coded by degenerated codon NNN, where N = A, G, C, T

Phenotypic Selection Based on Color Formation

About 10 ng mutant library plasmid DNA was used to transform competent *E. coli* BL21 (DE3) cells (Novagen, CA, USA) by a standard protocol [18]. A portion of 200 μl from each *E. coli* BL21 (DE3) transformation was plated on agar plates and incubated overnight at 37 °C and then were placed into cold room (16 °C) until blue positive colonies appeared.

Library Screening

Each blue colony was picked from the agar plates and placed into 200 μl LB broth supplemented with kanamycin for selection (30 μg/ml) in 96-well plates (master plates). Enzyme expression was performed in 1.2-ml deep-well plates containing 600 μl Luria–Bertani medium supplemented with kanamycin (30 μg/ml). Cells were grown at 37 °C and 200 rpm and induced with 0.5 mM IPTG at an OD_{578} 0.7–1.0. After incubation at 30 °C and 200 rpm for 12–16 h, the cells were collected by centrifugation at 3,220×*g* for 30 min, treated with lysozyme (1 mg/ml) and DNAse (1 μg/ml), and then frozen and thawed. The crude cell extracts were obtained by centrifugation at 14,000 rpm for 10 min, and the supernatant was used for the activity assay in the primary screening. About 180 μl supernatant aliquots were transferred into new 96-well plates for screening. Indole (200 μM) in DMSO (1%) was added to the lysate, and the plates were incubated for 10 min at room temperature before NADPH (500 μM) solution was added. Indigo production were measured at room temperature at 670 nm 30 min using FLUO star 403 spectrophotometer (BMG Lab Technologie, NC, USA), and product concentration was calculated using ε=3,900 $M^{-1}\cdot cm^{-1}$. In parallel, NADPH (500 μM) consumption rate was measured at room temperature at 340 nm and calculated using ε=6,200 $M^{-1}\cdot cm^{-1}$. The background signal originating from the NADPH oxidation without addition of the substrate served as a negative control.

Protein Expression and Purification

Protein expression and purification were performed as previously described [20]. Concentration of correctly folded P450 enzymes was determined from the CO-difference spectra of the reduced heme iron as reported elsewhere [21].

Determination of Kinetic Parameters

The assay was carried out in preparations containing 10–250 mM indole solution in DMSO (10 μl), 100 mM Tris–HCl buffer (850 μl) and parent-type and mutated P450 BM-3 (0.6 nmol) in a final volume of 1 ml. Kinetic constants were determined using indigo assay [11], and all values were measured at least in triplicates. The Michaelis–Menten parameters were determined by standard methods.

NADPH Consumption Assay

The NADPH consumption assay was performed as described elsewhere [14]. The observed rates of NADPH consumption were corrected for the slow background reaction that was observed with substrate but without enzyme.

Product Analysis by HPLC

Purified enzymes (2.4 μM P450) were incubated with 10 mM indole in DMSO (1%) in 100 mM Tris–HCl buffer, pH 8.2 for 10 min at room temperature before the NADPH (500 μM) solution was added. Aliquots were taken at zero and 120 min, and 3-methylindole (10 μg) was added before extraction as an internal standard. Products were extracted with CH_2Cl_2, air-dried, dissolved in a 15% CH_3CN in 50 mM Tris–HCl (pH 7.5, *v*/*v*), and injected onto a Hypersil ODS C18 reverse-phase column (4.6×250 mm, Aglient 2100 system). The column was eluted at a flow rate of 1 ml/min with the following gradient: 0–15 min: 15% CH_3CN, 85% 50 mM potassium phosphate, pH 7.5; 15–30 min: 15 to 40% CH_3CN gradient; 30–40 min: 40 to 50% CH_3CN gradient; 40 to 45 min: 50 to 15% CH_3CN gradient; 45–55 min: isocratic with 15% CH_3CN (all *v*/*v*). Retention time was determined using authentic references: indole, Rt 34.7 min; indirubin, Rt 38.4 min; indigo Rt 42.5 min.

Protein Modeling

Modeling of the P450 BM-3 enzyme was guided by the structure of P450 BM-3 obtained from the Protein Data Bank [22, 23]. Models of the P450 BM-3 mutants were created by the program Swiss PDB using the structure of P450 BM-3 PDB ID: 1BVY) as a template [24]. As substrate's molecule, a model of indole was created using the molecule builder of SYBYL.

Results

Random Mutagenesis for Higher Activity of P450 BM-3 on Indole

The triple mutant of P450 BM-3(A74G/F87V/L188Q) has previously been demonstrated to hydroxylate indole producing indigo and indirubin. For further improvement of the enzyme activity towards indole, error-prone PCR was performed. After one round of random mutagenesis, five mutant libraries were produced by error-prone PCR with different mutagenic factors. A convenient colorimetric colony-based method based on the known ability of the triple mutant to oxidize endogenous indole to indigo in vivo was adopted for the primary screening, resulting in macroscopic blue colonies [11]. The color of colonies was dependent on enzyme activity and protein expression. This approach allowed rapid visual screening of thousands of colonies on LB plates without addition of exogenous indole.

To identify the influence of $MnCl_2$ concentration on the mutagenic efficiency, the ratio of blue "active" colonies on each library to the total number of colonies was calculated. It was found that the amount of blue colonies decreased as the concentration of mutagenic factor $MnCl_2$ increased. The fraction of blue colonies reached 40% in the library created by adding 0.05 mM $MnCl_2$ during error-prone PCR. No blue colonies were found when the concentration of mutagenic factor $MnCl_2$ was 0.2 mM. With 0.10 mM and 0.15 mM $MnCl_2$, the fraction of colonies with blue color could reach 17 and 5%, respectively.

The secondary screening was performed in microtiter plates. Li et al. [11] reported that enzyme activity assay can easily be measured by monitoring indigo production at 670 nm at 1 ml-scale or larger scale. Here, all reaction components in the indigo-assay method constructed by Li were downscaled to fit the 96-well plate scale. In parallel, NADPH assay in microtiter plates was also applied as a complement to indigo assay lessening the screening error.

Through the iterative screenings from a total of approximately 6,000 colonies produced by error-prone PCR, several candidates were chosen and subsequently characterized by nucleotide sequence analysis, as shown in Table 2. Sequence analysis revealed two mutants with one additional amino acid substitution, K434R and E435D, respectively, and one mutant with three additional amino acid substitutions D168N, A225V, and K440N.

Kinetic parameters (Table 2) demonstrated that three mutants had higher catalytic activities towards indole than the parental enzyme. The mutant 3X/D168N/A225V/K440N was most efficient (125 $min^{-1}{\cdot}mM^{-1}$ vs 78 $min^{-1}{\cdot}mM^{-1}$). Although no dramatic enhancement of activity was observed during indole oxidation catalyzed by the new mutants, the reduced K_m values reflected higher affinities of these enzymes to indole.

Identification of a Critical Residue Using Saturation Site-Directed Mutagenesis

For the further improvement of enzyme activity and the identification of the target residues, five libraries were created using site-directed saturation mutagenesis at amino acid positions 225, 168, 434, 435, 440, respectively. The blue active colonies were randomly picked and analyzed according to the aforementioned screening procedure. About 1,000 colonies from five libraries were investigated in 96-well microtiter plates. Thirty-five colonies with higher activity during screening were subjected to DNA sequence analysis. Lastly, only 12 mutants were revealed with amino acid alterations. To quantify these mutants in detail, production of indigo was assayed individually at 670 nm using crude extracts (0.6 μM P450 BM-3) and 2 mM substrate concentration (Fig. 1a, b).

Figure 1b showed that four mutants 3X/A225P, 3X/A225Q, 3X/A225F, and 3X/A225G had approximately the same activity as the parental enzyme even if amino acids proline, glutamic acid were largely different from the original amino acid ananine considering their polarities, structures etc., which could illuminate that amino acid in position 225 played a null role in the relationship between structure and function of P450 BM-3.

A set of single mutation in position 440 has not been found by saturation mutagenesis although thousands of colonies were screened. Until now, we cannot deduce what kind of role position 440 played in hydroxylating indole. The further experiment is in progress to validate the 440 position effect.

Three other mutants (3X/D168H, 3X/K434G, 3X/E435T) with distinctly changed activities (Fig. 1a, b), which were confirmed several times in parallel experiments, were purified by Ni-NTA to measure kinetic parameters. Synchronously, a model was constructed on the basis of the X-ray structure of P450 BM-3 and indole was docked in the binding pocket (Fig. 2). The positions of the mutated amino acids and the heme were indicated, as shown in Fig. 2. Kinetic parameters of mutants 3X/D168H, 3X/E435T, and 3X/K434G were summarized in Table 3.

Table 2 Kinetic parameters of P450 BM-3 mutants constructed by error -prone PCR in reaction with indole.

P450 BM-3 mutants	K_m (mM)	k_{ca} (min^{-1})	k_{cat}/K_m(min^{-1} mM^{-1})	Coupling efficiency (%)
WT	nd	nd	nd	nd
3X	2.2	171	78	18
3X/E435D	1.9	178	104	20
3X/D168NA225VK440N	1.5	187	125	27
3X/K434R	2.0	175	87	18

3X The triple mutant A74G/F87V/L188Q, *nd* not detectable

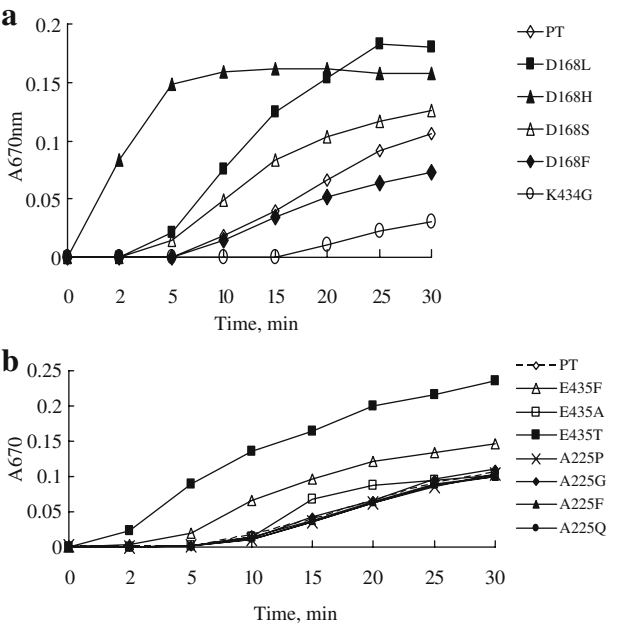

Fig. 1 In vitro formation of a blue pigment indigo by different P450 BM-3 mutants (crude extract). In all cases, (**a**, **b**) 2 mM indole was incubated with 0.6 μM P450 at 25°C for 30 min, and dye production was analyzed by measuring absorption at 670 nm

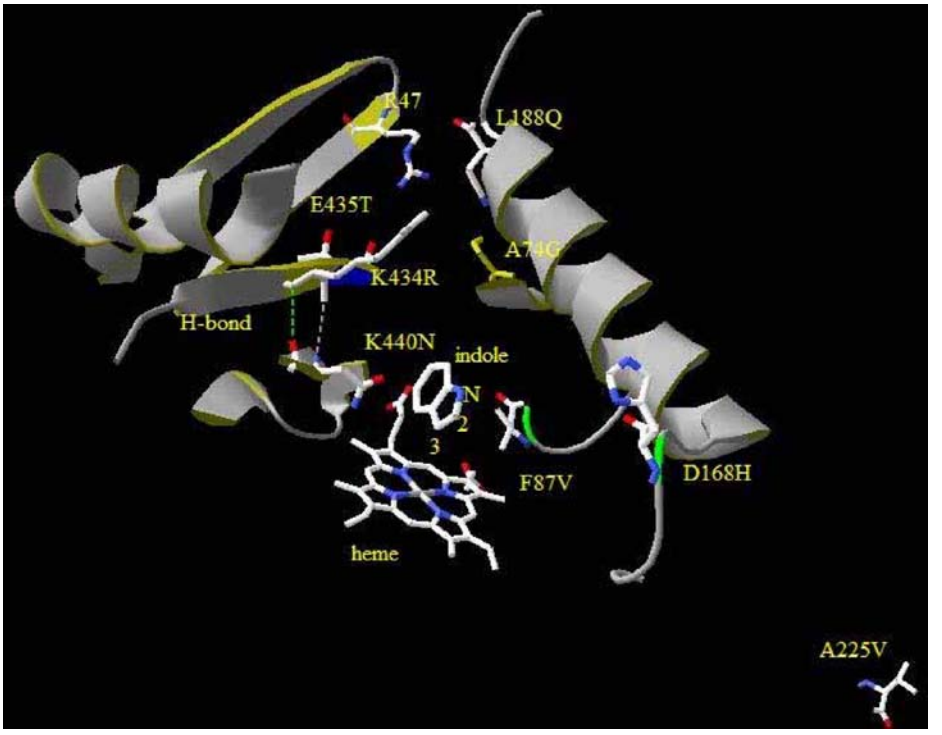

Fig. 2 Model of P450 BM-3 with indole bound. Mutations sites are shown. The heme is visible in the *lower left* corner

Two mutations, D168H and E435T, led to a further increase of k_{cat} value. And a highest affinity (0.8 mM) and catalytic efficiency (563 $min^{-1} \cdot mM^{-1}$) were observed in mutant 3X/E435T (Tables 2 and 3). Mutation K434G led even to a remarkable decrease in activity, although the 3X/K434R mutant evolved by error-prone PCR showed a slightly increased catalytic efficiency (Table 2). A reasonable explanation could be supposed that a basic arginine or lysine at position 434 is more beneficial for enzyme activity than a small uncharged glycine.

In general, all the mutants had quite low coupling efficiencies (8–27%) between NADPH oxidation and indole hydroxylation. For the mutant 3X/D168H, the NADPH oxidation rate was almost improved eightfold faster than that of the parental enzyme, whereas its indole-hydroxylating activity was increased only threefold (600 min^{-1} vs 171 min^{-1}; Table 2). The lowest coupling efficiency and highest hydroxylation activity of the mutant 3X/D168H among all of mutants engineered in this paper can hardly be explained from the model, as position 168 was located on the surface of the protein molecule and cannot affect activity or substrate binding directly (Fig. 2).

Determination of Enzyme Regioselectivity

Indigo was product of oxidative dimerization of two 3-hydroxyindole molecules, whereas indirubin was formed when both 2- and 3-hydroxyindole were produced during indole oxidation. To determine regioselectivity of each mutant (3X/D168H, 3X/K434G, 3X/E435T), 2.4 nmol purified enzymes were applied to hydroxylate indole and produce sufficient amount of the hydroxylated product. Comparison of the high-performance liquid chromatography (HPLC) profiles of the products (monitored at 240 nm) revealed significant differences among P450 BM-3 mutants. The mutation D168H influenced the regioselectivity of the triple mutant. A main product 3-hydroxyindole was built, leading to indigo (93%) and indirubin (7%), whereas the parental enzyme produced 72% indigo and 28% indirubin. Hisitidine at position 168 was speculated to force the change of indole orientation in the binding pocket. A change of regioselectivity was observed also when another variant E435T was introduced into the triple mutant. In this case, the reaction resulted also mainly in indigo (85%). In amino acid 435, the glutamic acid was replaced by threonine, which might cause a conformational change of in the region of substrate entrance. In both cases, the acidic amino acid residues (aspartic acid and glutamic acid, respectively) at D168H and E435T had been replaced by the basic (histidine) or neutral (threonine) amino acid.

Table 3 Kinetic parameters and product ratio of P450 BM-3 mutants constructed by saturation site-directed mutagenesis.

P450 BM-3 Mutants[a]	K_m (mM)	k_{cat} (min^{-1})	k_{cat}/K_m (min^{-1} mM^{-1})	Indigo[b] (%)	Indirubin[b] (%)	Coupling efficiency (%)
3X	2.2	171	78	72	28	18
3X/D168H	1.2	600	500	93	7	8
3X/K434G	3.9	87	22	77	23	12
3X/E435T	0.8	450	563	85	15	26

3X The triple mutant A74G/F87V/L188Q

[a] P450BM-3 mutants were purified

[b] Product ratio in % of product mixture

Discussion

In this study, directed evolution was employed to enhance the catalytic properties as well as the regioselectivity of P450 BM-3 in hydroxylating indole. The feasibility of a directed evolution depended on a facile screening assay to identify mutant colonies against a background of thousands normal variants. Herein, simple and rapid selections of mutants had been employed based on a colorimetric-colony assay on the agar plates in combination with two parallel spectrophotometric assays in 96-well plates. Using the combination of random mutagenesis and subsequent saturation mutagenesis with the described high throughput screening system, three residues 168, 434, 435 as the important amino acid position were identified. New P450 variants with higher activity toward indole acquired mutations that could not be predicted on the basis of rational design, pinpointing the power of directed evolution and aiding our further search for P450BM-3 variants with improved catalytic efficiency.

According to the modeling, E435 and K434 were located close to each other in the 3D structure and can form the hydrogen bonds with some amino acids at this domain. Glutamic acid substituted by threonine at position 435 directly or indirectly broke the hydrogen bonds between the relative amino acids at this domain, which may result in the improvement of the flexibility of the relative side chains at this domain because in induced-fit hypothesis by Daniel Koshland, perfect expression of catalytic activity of enzyme depends on the rapid change of the three dimensional structure of the active site [25]; thus, the highly flexible structure of proteins should be taken into account. Here, the introduction of threonine at position 435 may enhance the flexibility of the enzyme, which could conform the shape of the active site to the shape of the substrate and have a direct impact on the substrate binding rate and equilibrium constant.

The experiments led to a mutant 3X/D168H displaying an increased NADPH turnover rate, but highly uncoupled indole hydroxylation (Table 3). Therefore, exchange at position 168 might influence the interaction between the monooxygenase domain and an FMN-binding reductase domain. Nevertheless, these assumptions were only provisional from models, although the mutants 3X/D168H, 3X/E435T, 3X/K434G had dramatic effects.

The regioselectivity of P450 BM-3 during indole hydroxylation was still an arduous challenge for the protein engineering because mutants producing indigo as a single pigment have not been found. But the evolved enzyme obtained in this study could serve as a template for further directed evolution. Moreover, the results obtained from this study may serve as a basis for further elucidation of the mechanism of substrate activation by P450 BM-3. An area of much current interest in P450 BM-3 is the combination of random mutagenesis and rational design to expand and to focus on the potential of P450 BM-3 enzyme in the catalysis of industrial preparations and production of new chemical compounds.

Acknowledgements This work was supported by the joint project of CSC (China)-DAAD (Germany) (2004c33036) and the National Natural Sciences Foundation of China (30570411).

References

1. Bayer, A. (1878). Synthese des Indigblaus. *Chemische Berichte, 11*, 1296–1297.
2. Heumann, K. (1890). Neue Synthese des Indigos und verwandter Farbstoffe 1. *Chemische Berichte, 23,* 3043–3045.
3. Koehler, C. S. W. (1999). Synthetic dyes and the German chemical industry. *Today's Chemist at Work, 8,* 85–94.

4. King, L. J., Parke, D. V., & Williams, R. T. (1966). The metabolism of [2-14C] indole in the rat. *Biochemistry Journal, 98,* 266–277.
5. Russell, G. A., & Kaupp, G. (1969). Oxidation of carbanions. IV. Oxidation of indoxyl to indigo in basic solution. *Journal of the American Chemical Society, 91,* 3851–3859.
6. Murdock, D., Ensley, B. D., Serdar, C., & Thalen, M. (1993). Construction of metabolic operons catalyzing the de novo biosynthesis of indigo in *Escherichia coli. Biotechnology, 11,* 381–386.
7. Ensley, B. D., Ratzkin, B. J., Osslund, T. D., Simon, M. J., Wackett, L. P., & Gibson, D. T. (1983). Expression of naphthalene oxidation genes in *Escherichia coli* results in the biosynthesis of indigo. *Science, 222,* 167–169.
8. Gillam, E. M. J., Aguinaldo, A. M., Notley, L. M., Kim, D., Mundkowski, R. G., Volkov, A. A., et al. (1999). Formation of indigo by recombinant mammalian cytochrome P450. *Biochemical and Biophysical Research Communications, 265,* 469–472.
9. Gillam, E. M. J., Notley, L. M., Cai, H., De Voss, J. J., & Guegerich, F. P. (2000). Oxidation of indole by cytochrome P450 enzymes. *Biochemistry, 39,* 13817–13824.
10. Nakamura, K., Martin, M. V., & Guengerich, F. P. (2001). Random mutagenesis of human cytochrome P450 2A6 and screening with indole oxidation products. *Archives of Biochemistry and Biophysics, 395,* 25–31.
11. Li, Q. S., Schwaneberg, U., Fischer, P., & Schmid, R. D. (2000). Directed evolution of the fatty-acid hydroxylase P450BM-3 into an indole-hydroxylating catalyst. *Chemistry- A European Journal, 6,* 1531–1536.
12. Narhi, L. O., & Fulco, A. J. (1986). Characterization of a catalytically self-sufficient 119,000-dalton cytochrome P-450 monooxygenase induced by barbiturates in *Bacillus megaterium. Journal of Biological Chemistry, 261,* 7160–7169.
13. Narhi, L. O., Wen, L. P., & Fulco, A. J. (1988). Characterization of the protein expressed in *Escherichia coli* by a recombinant plasmid containing the *Bacillus megaterium* cytochrome P-450 BM-3 gene. *Molecular and Cell Biochemistry, 79,* 63–71.
14. Appel, D., Lutz-Wahl, S., Fischer, P., Schwaneberg, U., & Schmid, R. D. (2001). A P450 BM-3 mutant hydroxylates alkanes, cycloalkanes, arenes and heteroarenes. *Journal of Biotechnology, 88,* 167–171.
15. Carmichael, A. B., & Wong, L. L. (2001). Protein engineering of *Bacillus megaterium* CYP102: the oxidation of polycyclic aromatic hydrocarbons. *European Journal of Biochemistry, 268,* 3117–3125.
16. Li, Q. S, Ogawa, J., Schmid, R. D., & Shimizu, S. (2001a). Engineering cytochrome P450 BM-3 for oxidation of polycyclic aromatic hydrocarbons. *Applied Environmental Microbiology, 67,* 5735–5739.
17. Peters, M. W., Meinhold, P., Glieder, A., & Arnold, F. H. (2003). Regio- and enantioselective alkane hydroxylation with engineered cytochromesP450 BM-3. *Journal of the American Chemical Society, 125,* 13442–13450.
18. Sambook, J., & Russell, D. W. (2001). *Molecular cloning: a laboratory manual*, 3rd edn. New York: Cold Spring Harbor Laboratory.
19. Vandeyar, M. A., Weiner, M. P., Hutton, C. J., & Batt, C. A. (1988). A simple and rapid method forthe selection of oligodeoxynucleotide-directed mutants. *Gene, 65,* 129–133.
20. Maurer, S., Schulze, H., Schmid, R. D., & Urlacher, V. B. (2003). Immobilisation of P450BM-3 andan NADP+ cofactor recycling system: towards a technical application of heme-containing monooxygenases in fine chemical synthesis. *Advanced Synthesis and Catalysis, 345,* 802–810.
21. Omura, T., & Sato, R. J. (1964). The carbon monoxide-binding pigment of liver microsomes. I. Evidence for its hemoprotein nature. *Journal of Biological Chemistry, 239*, 2370–2378.
22. Bernstein, F. C., Koetzle, T. F., Williams, G. J. B., Meyer, J. E. F., Jr., Brice, M. D., Rodgers, J. R., et al. (1977). The protein data bank: A computer-based archivalle for macromolecular structures. *Journal of Molecular Biology, 112,* 535–542.
23. Gunsteren, W. F. van., Billeter, S. R., Eising, A. A., Hünenberger, P. H., Krüger, R., Mark, A. E., et al. (1996). In biomolecular simulation: The gromos96 manual and user guide. Vdf, Hochschulverlag an der ETH; BIOMOS.
24. Sevrioukova, I. F., Li, H., Zhang, H., Peterson, J. A., & Poulos, T. L. (1999). Structure of a cytochrome P450-redox partner electron-transfer complex. *Proceedings of the National Academy of Sciences, 96,* 1863–1868.
25. McKee, T., & McKee, J. R. (2001). *Biochemistry.* McGraw-Hill, pp. 121–122.